

High-Pressure Synthesis of YScO_3 , HoScO_3 , ErScO_3 , and TmScO_3 , and a Reevaluation of the Lattice Constants of the Rare Earth Scandates

J. B. CLARK, P. W. RICHTER, AND L. DU TOIT

National Physical Research Laboratory, South African Council for Scientific and Industrial Research, P.O. Box 395, Pretoria 0001, South Africa

Received March 29, 1977; in revised form June 20, 1977

The rare earth scandates $A\text{ScO}_3$ where $A = \text{Y, La, Nd, Sm, Gd, Dy, Ho, Er, and Tm}$ have been prepared and their unit-cell constants determined. The single-phase compounds YScO_3 , HoScO_3 , ErScO_3 , and TmScO_3 have been prepared for the first time using high pressures.

Introduction

A large amount of work has been done on the synthesis and crystallographic properties of rare earth scandates, vanadates, galliates, orthochromites, aluminates, and especially orthoferrites (1). Most of the perovskite-like compounds in this series are isostructural with GdFeO_3 (2), which consists of four GdFeO_3 distorted perovskite units in an orthorhombic unit cell with space group $D_{2h}^{16}-Pbnm$. The structure consists of corner-shared octahedra where the cooperative buckling of these octahedra leads to the orthorhombic distortion. The interest shown in these compounds has been due to their interesting physical properties, in particular magnetic properties.

Earlier reports on compounds in the systems $\text{Ln}_2\text{O}_3\text{-Sc}_2\text{O}_3$ ($\text{Ln} = \text{Y, La, Pr, Nd, Sm, Eu, Gd, Tb, Dy, Ho, Er, Tm, Yb, Lu}$) are those of Keith and Roy (3), who produced partial formation of LaScO_3 and NdScO_3 ; Geller (4), who presented crystallographic data on LaScO_3 , PrScO_3 , NdScO_3 , GdScO_3 and YScO_3 ; Schneider *et al.* (5) who presented synthesis and crystallographic information on the pure perovskites SmScO_3 ,

EuScO_3 , GdScO_3 , and DyScO_3 and information on the partial formation of the perovskites HoScO_3 and YScO_3 at reaction temperatures as high as 1900°C . They also reported that no perovskite formation took place for $\text{Ln} = \text{Er, Yb, Lu}$. Instead, cubic solid solutions were formed. More recently Badie and co-workers (6-8) have reported high-temperature studies on LaScO_3 , NdScO_3 and the compounds Dy_3ScO_6 , Ho_3ScO_6 , and Y_3ScO_6 . Comprehensive powder data have recently been presented for EuScO_3 (9).

The method most used for predicting the possible stability of perovskites has been the Goldschmidt (10) tolerance factor

$$t = \frac{r_A + r_X}{2^{1/2}(r_B + r_X)}$$

where r_A , r_B , and r_X are the empirical ionic radii of the respective ions in the compound ABX_3 . The perovskite structure occurs within the range $0.75 < t < 1.00$. For $t = 1$ the ideal cubic perovskite structure occurs, and as t decreases the unit cell shows a fourfold increase in volume as it enlarges to accommodate the distortion caused by the buckling

TABLE I

Compound	Goldschmidt tolerance factor	Ionic radius ^a RE_{IX}^{3+}
LaScO ₃	0.863	1.216
PrScO ₃	0.850	1.179
NdScO ₃	0.845	1.163
SmScO ₃	0.835	1.132
EuScO ₃	0.831	1.120
GdScO ₃	0.827	1.107
TbScO ₃	0.823	1.095
DyScO ₃	0.819	1.083
YScO ₃	0.816	1.075
HoScO ₃	0.815	1.072
ErScO ₃	0.812	1.062
TmScO ₃	0.808	1.052
YbScO ₃	0.805	1.042
LuScO ₃	0.802	1.032

^a Radii were taken from Shannon (11). Ideally the *A* atoms in the *AScO*₃ compounds are 12-fold coordinated. No data are available for RE_{XII}^{3+} so we have used the largest observed values for the *A* cations, i.e., 9-fold coordinated. Values of $Sc_{VI}^{3+} = 0.745$ Å and $O^{2-} = 1.40$ Å are used (11).

of the corner-shared octahedra. Table I shows the calculated tolerance factors for the present series of compounds. According to the above criterion all these compounds should yield perovskites, but from Schneider *et al.* (5) it is apparent that certain compounds prefer *C*-type solid solutions where the preference for both *A* and *B* atoms to be in octahedral sites becomes predominant. The *C*-type *M*₂O₃ structure consists of two types of corner-shared six-coordinated sites.

Pressure is known to favor higher-coordinated sites, and for this reason it was expected that high-pressure synthesis conditions could force compounds with lower tolerance factors to adopt the perovskite structure. In particular, equimolar mixtures of the constituent oxides having the expected general formulas YScO₃, DyScO₃, HoScO₃, ErScO₃, TmScO₃, YbScO₃, and LuScO₃ were studied at high pressures.

Experimental

All oxides used in the present study were obtained from Koch-Light and had stated purities of 99.9% with the exception of Sc₂O₃, which had a stated purity of 99.6%. Equimolar mixtures of Sc₂O₃ and the rare earth oxide concerned were thoroughly ground and pellets were pressed at ~5 kbar in a pill press. The pellets were placed in a furnace and heated in air at 1600°C in a Pt 10% Rh crucible for 12 hr.

The compounds that did not yield pure perovskites after this treatment at atmospheric pressure were then treated at high pressures as follows. Samples were sealed in platinum tubes which were then subjected to quasi-hydrostatic pressures in a piston-cylinder device (12). The tubes were fitted into holes drilled in boron nitride cylinders, which were then placed in a conventional talc or pyrophyllite oven assembly. Pressures quoted were only approximately corrected for the various effects present in such systems (13) and are thought to be correct to within ±2 kbar. Temperatures were determined from previously determined calibration curves of wattage versus temperature and are correct to within ±20°C. In all cases pressure was applied to within ~2 kbar of the quoted values before temperature was raised. Once the desired reaction temperature was reached, pressure was raised to the final value. The reaction conditions were maintained for 1 hr and then temperature was dropped by switching off the heating current and finally pressure was released when the temperature was ~30°C.

X-Ray powder diffraction patterns were recorded on a Huber Guinier camera using monochromatized $CuK\alpha_1$ radiation ($\lambda = 1.54051$ Å). Si was used as an internal calibrant and both film and counter techniques were employed. The angular zone for $2\theta < 90^\circ$ was recorded using the asymmetric transmission mode while the zone $2\theta \geq 90^\circ$ was recorded using the asymmetric back reflection mode.

TABLE II

Composition of final product	Product after heating equimolar mixtures in air at 1600°C for 60 hr	Product after 1 hr at 20 kbar 1000°C	Product after 1 hr at 30 kbar 1000°C
LaScO ₃	Perovskite	—	—
NdScO ₃	Perovskite	—	—
SmScO ₃	Perovskite	—	—
GdScO ₃	Perovskite	—	—
YScO ₃	C-type solid solution plus trace of perovskite	Perovskite	—
DyScO ₃	C-type solid solution plus perovskite	Perovskite	—
HoScO ₃	C-type solid solution plus perovskite	Perovskite	—
ErScO ₃	C-type solid solution	Perovskite	—
TmScO ₃	C-type solid solution	Perovskite	—
YbScO ₃	C-type solid solution	C-type solid solution	C-type solid solution
LuScO ₃	C-type solid solution	C-type solid solution	C-type solid solution

Results

The results obtained are shown in Table II. The results after firing in air at atmospheric pressure are in good agreement with Schneider *et al.* (5). Of the remaining equimolar mixtures that did not yield single-phase perovskites, viz, YScO₃, DyScO₃, HoScO₃, ErScO₃, TmScO₃, YbScO₃, and LuScO₃, treatment at 20 kbar 1000°C for 1 hr was sufficient to yield pure perovskites for YScO₃, DyScO₃, HoScO₃, ErScO₃, and TmScO₃. The resulting solid solutions of the Yb and Lu compounds were further treated at 30 kbar, 1000°C for 1 hr, but they remained cubic solid solutions with slight evidence of a possible further phase in both cases. The new phase, although very difficult to detect, did not appear to be the expected perovskite.

Table III lists the lattice parameters of all perovskites formed in the present study. The data for TmScO₃ is presented in Table IV. The powder data for the series of compounds was generally similar and in most cases some 100 reflections were reliably indexed. Notable exceptions were GdScO₃ and SmScO₃ where fluorescence effects raised the background radiation obscuring weak reflections. In these cases the high-angle peaks ($2\theta > 90^\circ$) were weak and difficult to measure and consequently only ~50 peaks were used in the refinement of their unit-cell constants.

TABLE III

Compound	Orthorhombic lattice parameters		
	<i>a</i> (Å)	<i>b</i> (Å)	<i>c</i> (Å)
LaScO ₃	5.6748	5.7911	8.0923
NdScO ₃	5.5772	5.7754	8.0037
SmScO ₃	5.5294	5.7599	7.9611
GdScO ₃	5.4908	5.7559	7.9382
DyScO ₃	5.4490	5.7273	7.9116
YScO ₃	5.4230	5.7091	7.8907
HoScO ₃	5.4226	5.7117	7.8904
ErScO ₃	5.4071	5.6985	7.8852
TmScO ₃	5.3913	5.6808	7.8860

Discussion

Figure 1 shows the lattice cell constants as a function of the ionic radius of the rare earth ion. Two distinct features are evident. For TmScO₃, ErScO₃, and HoScO₃ the *c* lattice constants are practically equal. To check this feature, tentative values for *c* were obtained by a smooth extrapolation of the data in Fig. 1. When these lattice constants were used to generate a set of *d* values no reliable indexing was obtained. Furthermore, if the data were then refined in four least-squares cycles, the original lattice constants were immediately regained and the data reliably indexed.

The second feature of the data is the overall tendency for *a* to increase sharply from Tm to

TABLE IV
 CRYSTALLOGRAPHIC DATA FOR TmScO_3

hkl	$d_{\text{obs}} (\text{\AA})$	$d_{\text{calc}} (\text{\AA})$	I_{obs}	hkl	$d_{\text{obs}} (\text{\AA})$	$d_{\text{calc}} (\text{\AA})$	I_{obs}
1 0 1	4.445	4.451	3	3 1 4	1.2930	1.2933	2
0 0 2	3.940	3.943	18	3 3 1	1.2860	1.2861	4
1 1 0	3.905	3.911	31	4 0 2	1.2752	1.2754	1
1 1 1	3.500	3.503	22	2 4 0	1.2564	1.2565	0.5
0 2 0	2.836	2.840	23	0 4 3	1.2499	1.2495	2
1 1 2	2.777	2.777	100	1 1 6	1.2462	1.2459	5
2 0 0	2.6930	2.6957	22	2 4 1	1.2411	1.2408	6
0 2 1	2.6704	2.6723	13	3 3 2	1.2380	1.2377	2
2 1 0	2.4326	2.4354	1	2 2 5	1.2279	1.2276	3
1 0 3	2.3617	2.3628	1	4 2 0	1.2179	1.2177	2
2 1 1	2.3264	2.3270	6	4 2 1	1.2037	1.2034	3
0 2 2	2.3041	2.3047	9	2 4 2	1.1976	1.1972	1
2 0 2	2.2244	2.2253	12	1 3 5	1.1823	1.1824	4
1 1 3	2.1811	2.1816	9	4 1 3	1.1737	1.1735	1
1 2 2	2.1190	2.1192	2	3 3 3	1.1680	1.1678	4
2 1 2	2.0709	2.0720	1	4 2 2	1.1636	1.1635	1
0 0 4	1.9709	1.9715	12	3 1 5	1.1605	1.1604	0.5
2 2 0	1.9541	1.9553	20	2 4 3	1.1337	1.1336	5
0 2 3	1.9286	1.9293	8	4 0 4	1.1124	1.1127	2
2 2 1	1.8975	1.8978	15	4 2 3	1.1046	1.1049	2
1 2 3	1.8165	1.8165	1	1 5 1	1.1009	1.1009	5
2 1 3	1.7865	1.7865	1	2 2 6	1.0908	1.0908	1
1 1 4	1.7606	1.7605	5	1 1 7	1.0822	1.0826	1
3 0 1	1.7521	1.7522	3	3 4 2	1.0722	1.0723	1
1 3 1	1.7421	1.7424	21	5 0 1	1.0683	1.0683	1
3 1 0	1.7137	1.7134	3	1 3 6	1.0585	1.0587	2
3 1 1	1.6752	1.6744	3	0 4 5	1.0553	1.0554	2
1 3 2	1.6279	1.6273	8	2 5 0	1.0471	1.0470	1
0 2 4	1.6203	1.6196	7	3 1 6	1.0428	1.0429	3
2 0 4	1.5915	1.5913	8	4 2 4	1.0362	1.0360	2
3 1 2	1.5715	1.5715	23	1 5 3	1.0240	1.0239	2
2 2 3	1.5691	1.5689	5	4 1 5	1.0083	1.0084	0.5
1 2 4	1.5504	1.5511	0.5	3 3 5	1.0048	1.0048	1
3 2 0	1.5185	1.5187	1	5 2 1	0.9998	0.9999	0.5
3 2 1	1.4912	1.4913	1	5 0 3	0.9974	0.9976	0.5
3 0 3	1.4831	1.4836	0.5	0 0 8	0.9856	0.9858	1
1 3 3	1.4773	1.4776	8	5 1 3	0.9827	0.9826	1
1 1 5	1.4623	1.4627	1	2 2 7	0.9763	0.9762	0.5
3 1 3	1.4349	1.4354	0.5	4 4 1	0.9702	0.9702	2
0 4 0	1.4200	1.4202	0.2	1 5 4	0.9683	0.9684	1
3 2 2	1.4165	1.4172	0.5	4 2 5	0.9638	0.9639	0.5
0 4 1	1.3972	1.3977	6	3 5 0	0.9602	0.9603	0.5
2 2 4	1.3879	1.3883	8	1 1 8	0.9557	0.9559	0.5
0 2 5	1.3783	1.3789	2	1 3 7	0.9529	0.9529	2
1 4 0	1.3727	1.3734	1	4 0 6	0.9411	0.9410	0.5
4 0 0	1.3474	1.3478	3	0 2 8	0.9312	0.9313	2
2 3 3	1.3351	1.3349	0.5	3 3 6	0.9255	0.9255	2
2 1 5	1.3233	1.3238	1	0 6 2	0.9205	0.9206	0.5
0 0 6	1.3142	1.3144	1	4 4 3	0.9161	0.9163	1
4 1 0	1.3112	1.3114	0.5	5 3 2	0.9114	0.9116	0.5

TABLE IV (continued)

hkl	d_{obs} (Å)	d_{calc} (Å)	I_{obs}	hkl	d_{obs} (Å)	d_{calc} (Å)	I_{obs}
1 5 5	0.9086	0.9087	1	4 4 5	0.8310	0.8310	1
3 5 3	0.9019	0.9020	1	3 2 8	0.8269	0.8269	0.2
6 0 0	0.8984	0.8986	0.5	5 1 6	0.8248	0.8248	1
6 1 0	0.8875	0.8875	1	3 5 5	0.8203	0.8203	0.2
0 4 7	0.8824	0.8826	1	6 0 4	0.8177	0.8176	0.5
2 2 8	0.8800	0.8802	1	6 2 3	0.8146	0.8145	0.5
1 4 7	0.8710	0.8710	0.5	5 3 5	0.8058	0.8056	0.5
1 3 8	0.8631	0.8631	0.5	1 7 0	0.8025	0.8025	1
4 1 7	0.8545	0.8546	0.5	1 5 7	0.7914	0.7913	0.5
3 3 7	0.8522	0.8524	0.5	1 3 9	0.7868	0.7867	0.5
2 4 7	0.8388	0.8388	1	6 2 4	0.7857	0.7857	0.2

Gd after which the rate of increase decreases substantially. This behavior is similar to that found for the rare earth orthorhodontes by Shannon (14). It was explained in terms of a regular increase in the average $A-O$ distance of the eight first nearest neighbors and a decrease in the average $A-O$ distance of the four second-nearest neighbors as A increases from Lu to La, by Marezio *et al.* (15).

From the present work it appears that as one progresses through the series $A\text{ScO}_3$, where $A = \text{Y, La, } \dots, \text{Lu}$, it becomes

increasingly difficult to synthesize the perovskite. This factor is also reflected in the decreasing Goldschmidt tolerance factor (Table I). The hypothetical compounds YbScO_3 and LuScO_3 could not be prepared even after treatment at pressures as high as 30 kbar and temperatures of 1000°C . The question arises as to whether YbScO_3 and LuScO_3 will in fact become stable at even higher pressures, or whether the C -type solid solution will be preferred.

Let us consider the hypothetical perovskite

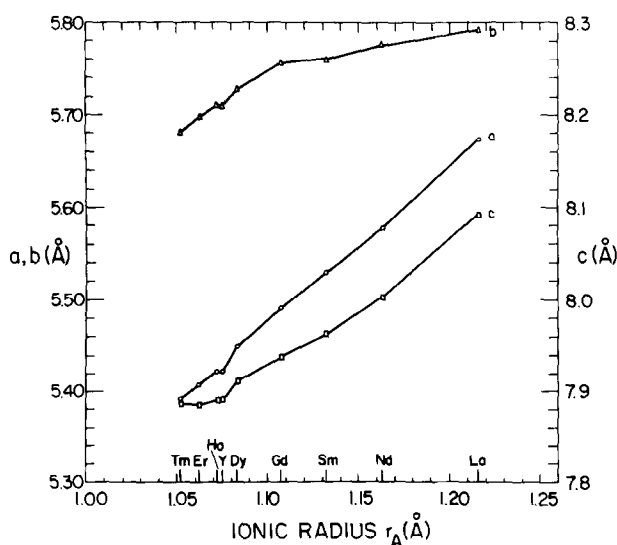


FIGURE 1

LuScO_3 . Extrapolating the present data for the series we can postulate an expected unit-cell volume of 237.4 \AA^3 for LuScO_3 . This represents a density of 7.5 g cm^{-3} . Using the present data it is possible to estimate that the *C*-type solid solution formed for $\text{Lu}_2\text{O}_3\text{-Sc}_2\text{O}_3$ has a unit-cell constant of $\sim 10.1 \text{ \AA}$ which implies a unit-cell volume of 1030 \AA^3 . From this we estimate a density of 6.9 g cm^{-3} . The perovskite unit cell therefore represents an attractive increase in density and must be preferred at higher pressure. Both Lu_2O_3 and Sc_2O_3 , however, adopt the monoclinic *B*-type rare earth oxide structure at higher pressures, and this factor could well complicate the picture considerably. Lu_2O_3 adopts the *B*-type structure at $\sim 40 \text{ kbar}$ and 1000°C (16). Sc_2O_3 does the same at 130 kbar , 1000°C (17). Sc_2O_3 remains *C*-type up to $\sim 110 \text{ kbar}$ where the *B*-type phase starts forming (17). There are therefore two distinct zones. Above 40 kbar Lu_2O_3 will occur in the *B*-type structure while Sc_2O_3 remains *C*-type. If we assume a mixture of these two phases, one can estimate the average density of the mixture as $\sim 7.0 \text{ g cm}^{-3}$ which is less than the density offered by the possible perovskite. Above $\sim 110 \text{ kbar}$, when Sc_2O_3 also starts transforming to the *B*-type structure, one can roughly estimate a density of $\sim 7.2 \text{ g cm}^{-3}$ for the mixture. This is still marginally lower than the calculated perovskite phase's density. From the above it would therefore be tentatively assumed that perovskite formation will occur for both the $\text{Lu}_2\text{O}_3\text{-Sc}_2\text{O}_3$ and $\text{Yb}_2\text{O}_3\text{-Sc}_2\text{O}_3$ systems at some higher pressure.

Acknowledgments

The authors would like to thank J. Erasmus and A. de Kleijn and their staff for technical maintenance. Calculations were carried out on the CDC 174 computer of the National Research Institute for Mathematical Sciences using a suite of programs from Professor K.-J. Range's laboratory at the University of Regensburg, Federal Republic of Germany. The programs were adapted by Mrs. M. C. Pistorius for use on the CDC 174.

References

1. An excellent review is to be found in Landolt-Börnstein, New Series, Group III: Crystal and Solid State Physics, Vol. 4, "Magnetic and Other Properties of Oxides and Related Compounds," (K.-H. Hellwege and A. M. Hellwege, Eds.), Part a, Springer-Verlag, Berlin (1970).
2. S. GELLER, *J. Chem. Phys.* **24**, 1236 (1956).
3. M. L. KEITH AND R. ROY, *Amer. Mineral* **39**, 1 (1954).
4. S. GELLER, *Acta Crystallogr.* **10**, 243 (1957).
5. S. J. SCHNEIDER, R. S. ROTH, AND J. L. WARING, *J. Research A* **65**, 345 (1961).
6. J. M. BADIE, *High Temp. High Press.* **2**, 309 (1970).
7. J. M. BADIE, J. COUTURES, A. ROUANET, AND M. FOEX, Etude des transformations cristallines à haute température, Colloques Internationaux C.N.R.S. (1972).
8. J. M. BADIE, *C.R. Acad. Sci. Ser. C* **277**, 1365 (1973).
9. M. FAUCHER AND P. CARO, *Mater. Res. Bull.* **10**, 1 (1975).
10. V. M. GOLDSCHMIDT, "Geochemische Verteilungsgesetze der Elemente VII, VIII" (1927/1928).
11. R. D. SHANNON, *Acta Crystallogr. Sect. A* **32**, 751 (1976).
12. G. C. KENNEDY AND P. N. LA MORI, in "Progress in Very High Pressure Research" (F. P. Bundy, W. R. Hibbard, and H. M. Strong, Eds.), Wiley, New York (1961).
13. C. W. F. T. PISTORIUS, E. RAPOPORT, AND J. B. CLARK, *Rev. Sci. Instrum.* **38**, 1741 (1967).
14. R. D. SHANNON, *Acta Crystallogr. Sect. B* **26**, 447 (1970).
15. M. MAREZIO, J. P. REMEIKA, AND P. D. DERNIER, *Inorg. Chem.* **7**, 1337 (1968).
16. H. R. HOEKSTRA, *Inorg. Chem.* **5**, 754 (1966).
17. A. F. REID AND A. E. RINGWOOD, *J. Geophys. Res.* **74**, 3238 (1969).